Highlights on Spanish Astrophysics IX, Proceedings of the XII Scientific Meeting of the Spanish Astronomical Society held on July 18 – 22, 2016, in Bilbao, Spain. S. Arribas, A. Alonso-Herrero, F. Figueras, C. Hernández-Monteagudo, A. Sánchez-Lavega, S. Pérez-Hoyos (eds.)

Dust emission in simulated dwarf galaxies using GRASIL-3D

I. M. Santos-Santos[1,2], R. Domínguez-Tenreiro[1,2], G. L. Granato[3], C. B. Brook[1,2] and A. Obreja[4]

[1] Depto. de Física Teórica, UAM, E-28049 Cantoblanco, Madrid, Spain
[2] Astro-UAM, UAM, Unidad Asociada CSIC, E-28049 Cantoblanco, Madrid, Spain
[3] Osservatorio Astronomico di Trieste, INAF, Via Tiepolo 11, I-34131 Trieste, Italy
[4] NYU Abu Dhabi, PO Box 129188, Saadiyat Island, Abu Dhabi, United Arab Emirates

Abstract

Recent *Herschel* observations of dwarf galaxies have shown a wide diversity in the shapes of their IR-submm spectral energy distributions as compared to more massive galaxies, presenting features that cannot be explained with the current models. In order to understand the physics driving these differences, we have computed the emission of a sample of simulated dwarf galaxies using the radiative transfer code GRASIL-3D. This code separately treats the radiative transfer in dust grains from molecular clouds and cirri. The simulated galaxies have masses ranging from $10^6 - 10^9$ $M_\odot$ and have evolved within a Local Group environment by using CLUES initial conditions. We show that their IR band luminosities are in agreement with observations, with their SEDs reproducing naturally the particular spectral features observed. We conclude that the GRASIL-3D two-component model gives a physical interpretation to the emission of dwarf galaxies, with molecular clouds (cirri) as the warm (cold) dust components needed to recover observational data.

1 Introduction

Dust emission from dwarf galaxies differs considerably from that of more metal-rich galaxies. Studies of their very diverse spectral energy distributions (SEDs) have shown that dwarfs harbour warmer dust [5], have lower dust-to-gas ratios [10] at given metallicities and show: i) lower polycyclic aromatic hydrocarbon (PAH) band emission, ii) IR peak broadening and iii) flattening of the FIR slope ("submm excess"). These results have been recently confirmed with the Dwarf Galaxy Survey (DGS) [9] and the *Herschel*-ATLAS Phase-1 Limited-Extent spatial Survey (HAPLESS) [1], both observed by *Herschel*. The nature of these features is still uncertain. While the SEDs of massive galaxies in the IR-submm range are typically fit

with models of modified blackbodies, in the case of dwarfs the inclusion of extra components, or the variation of parameters like the emissivity index β, is required to fit the data.

The aim of this study is to provide a physically based explanation to the particular emission features dwarf galaxies show in the IR-submm range. This will be done by studying the SEDs of a sample of simulated dwarf galaxies from the CLUES project, calculated using the GRASIL-3D radiative transfer code which treats separately the dense and the diffuse gas.

2 Methodology

GRASIL-3D We briefly recall the main features of GRASIL-3D [2]. The gas is subdivided in a dense phase (fraction f_{mc} of the total mass of gas) associated with young stars (star-forming molecular clouds, MCs) and a diffuse phase (cirrus) where more evolved (free) stars and MCs are placed. The MCs are represented as spherical clouds with optical depth $\tau \propto \delta\, m_{mc}/r_{mc}^2$ (where δ is the dust to gas mass ratio, m_{mc} is the mass of individual MCs, and r_{mc} is their radius), containing a central source, whose radiative transfer through MCs is calculated following [8]. The radiative transfer of the radiation emerging from MCs and from free stars is then computed through the cirrus dust. In GRASIL-3D the dust to gas mass ratio is a local quantity that changes in each grid cell. It has been taken to vary with metallicity following the broken power law proposed in Table 1 of [10], that provides a lower amount of dust to regions of lower metallicity. The f_{mc} fraction is calculated by implementing a sub-resolution model based on a theoretical log-normal probability distribution function (PDF) for the gas densities, and on the assumption that MCs are defined by a density threshold, $\rho_{mc,thres}$. This approach is sopported by small scale simulations [16] and observationally [12]. The disperson of the PDF σ, together with $\rho_{mc,thres}$ determine the mass in MCs.

The luminosity of the young stellar populations placed inside each MC is modelled by linearly decreasing the fraction f of stellar energy radiated inside the cloud with its age t:

$$f(t) = \begin{cases} 1 & t \le t_0 \\ 2 - t/t_0 & t_0 < t \le 2t_0 \\ 0 & t > 2t_0 \end{cases} \quad (1)$$

where t_0 is a parameter representing the time taken for stars to escape the MCs where they were born, and mimics MC destruction by young stars. Only stars with ages $< 2 \times t_0$ are eligible to form part of the MC heating engine. Observationally, t_0 takes values of the order of the lifetime of the most massive stars, 3-100 Myrs, and it varies with the density of the surrounding interstellar medium, being higher in the densest environments. Typical values were found by comparison to local observations in [13], yielding $\sim$ 2.5-8 Myrs for normal spiral galaxies, and 18-50 Myrs for starburst galaxies. The dust is assumed to consist of a mixture of silicate and graphite, where carbonaceous grains with size $< 100\mathring{A}$ are assumed to have PAHs properties, according to [4]. A different dust composition and size distribution is assumed for MCs and cirri. For cirrus, we have adopted a size distribution with a PAH abundance of $q_{\rm PAH} = 1.12\%$ [4], as suggested by observations of low metallicity galaxies [3]. For MCs, the dust model is taken from [13], updated by [15], with a 1000 times lower PAH abundance relative to the diffuse component to fit the SEDs of star forming galaxies.

The following set of parameters has been used here: t_0=40 Myrs; $\rho_{mc,thres} = 3.3 \times 10^9$ $M_\odot kpc^{-3}$; σ=2, though their variation (inside observational ranges) has been proved not to alter the final qualitative result of this work. We refer the reader to [2] for details.

The Simulation The sample of simulated dwarf galaxies used is from a single simulation with initial conditions from the Constrained Local UniversE Simulations (CLUES) project [1] [6], where observational data are imposed as constraints on the initial conditions in order to simulate a cosmological volume that is representative of our local universe. The mass resolution of particles is m_{star}=1.3×10^4 $M_\odot$, m_{gas}=1.8×10^4 $M_\odot$ and m_{dm}=2.9×10^5 $M_\odot$, and the gravitational softening lengths are ϵ_{bar}=223 pc between baryons and ϵ_{dm}=486 pc between dark matter particles. The cosmology used is ΛCDM with WMAP3 parameters. The hydrodynamical run has been done using the parallel N-body+SPH tree-code `GASOLINE` [17], which includes gas hydrodynamics and cooling, star formation, energy feedback and metal enrichment to model structure formation. See [14, 7] for details.

This CLUES simulation produced 120 galaxies ranging 10^6-10^9 $M_\odot$ in stellar mass, to which we asign the label "dwarf". Since we are interested in the IR-submm emission produced by the reemission of ultraviolet light absorbed by dust grains, we have focused on those dwarfs that have recent star formation; in particular, that contain stellar particles with ages smaller than 80 Myrs (t_0=40 Myrs). This leaves a final sample of 27 dwarf galaxies, which present differences in their star formation histories, stellar and gas masses, sizes and morphologies. A prior study has shown that all these properties are inside observational expectations, proving CLUES as a reliable Local Group simulation (Santos-Santos, in prep).

3 Results: The diversity of emission in the IR-submm range

In Fig. 1 we show the spectral energy distributions of the different simulated dwarfs calculated with GRASIL-3D, using the standard β=2. The intrinsic stellar emission is shown in red, the MC emission in blue, the cirri in green and the black curve gives the total SED emission. Thanks to the combined contribution of emission from MCs and cirri, they show a surprising variety and mimick the different characteristics seen in DGS and HAPLESS. Specific examples follow: galaxies #32, 34, 70, 149 show clear IR peak broadening, #26, 32, 50, 116 show a submm excess and flattening of the IR slope, and #32, 50, 104, 149 show very low PAH emission. The rest show mixed properties and finally there are some cases where none of these properties are apparent. We differentiate between 3 extremal behaviours with respect to the MC emission: i) MC emission dominates, hiding PAH emission and with maxima around 30 μm; ii) its intensity is similar to that of cirri, generating a flat region between both maxima; iii) it is very poor or inexistent, and we are left with only 1 component, that of cirri. To better quantify the comparisons with observations we have done a color-color analysis.

IR peak broadening The left panel of Fig. 2 shows the PACS/PACS $\nu L_{70}/\nu L_{100}$ vs $\nu L_{100}/\nu L_{160}$ color-color diagram, which traces the peak of the SED, or the global "temper-

[1] `http://clues-project.org/`

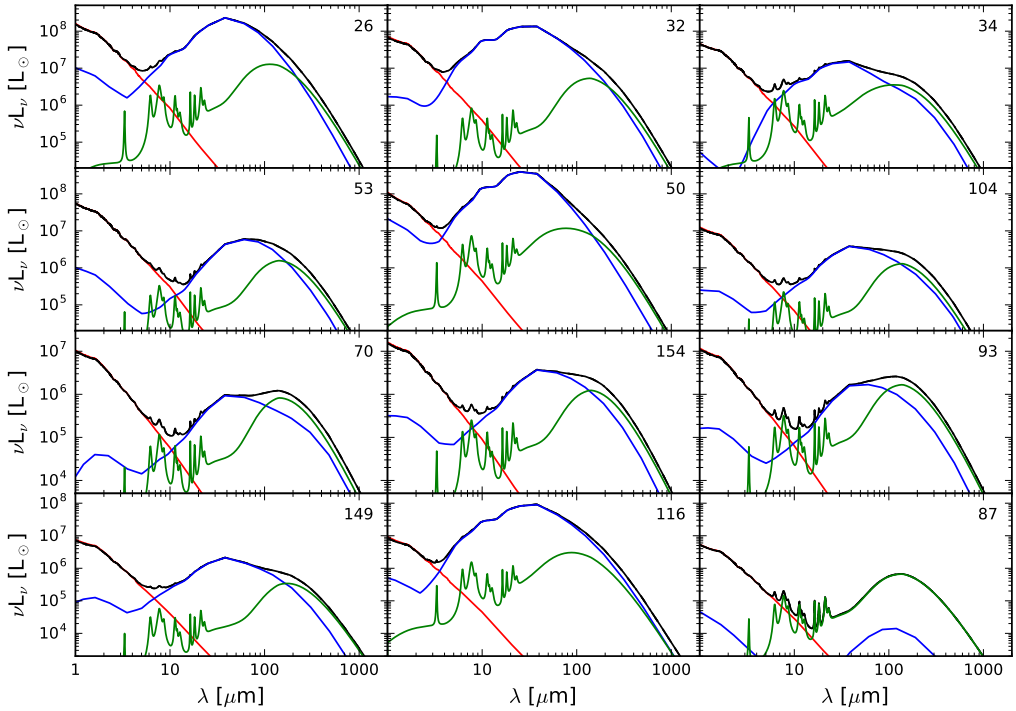

Figure 1: Spectral energy distributions of some representative CLUES star-forming dwarf galaxies. Red: intrinsic stellar emission; blue: emission from molecular clouds; green: emission from cirri; black: total dust affected SED.

ature" of the dust in the galaxy [9]. Gray crosses (DGS) and points (KINGFISH) stand for observational data, where faint (contrasting) symbols correspond to galaxies above (inside) the dwarf stellar mass range. Squares show the CLUES results colored by the ratio of the energy absorbed by MCs to the total MC dust mass.

High mass galaxies gather in the lower left corner of the figure where $\nu L_{70}/\nu L_{100} < 1$ and $\nu L_{100}/\nu L_{160} \sim 1$, because they peak at high λ. CLUES dwarf galaxies with no MC emission gather in this region too. On the other hand, dwarfs that show a maximum emission in the 20 - 40 μm range (MC emission dominance) have, $\nu L_{70}/\nu L_{100} > 1$ and $\nu L_{100}/\nu L_{160} > 1$, placing them in the upper right part of the diagram; and dwarfs showing a rather flat behaviour in the $\lambda \sim 40 - 160$ μm range are closer to the (1,1) position of the diagram. Note how CLUES dwarfs with high MC emission appear in the same region of the diagram as DGS galaxies whose SED data has been fit in [11] with an extra emission component as a MIR modified black body (circled data). Warmer temperatures of MC dust grains in CLUES dwarfs are due to the higher energy absorption of this dust per unit mass, as indicated by the colorbar. Indeed, if the energy input from young stars in MCs is lowered (i.e., lower t_0), the energy absorption by unit dust mass therein decreases, and consequently its emission becomes colder (their color changes to dark blue and they move towards the lower left corner).

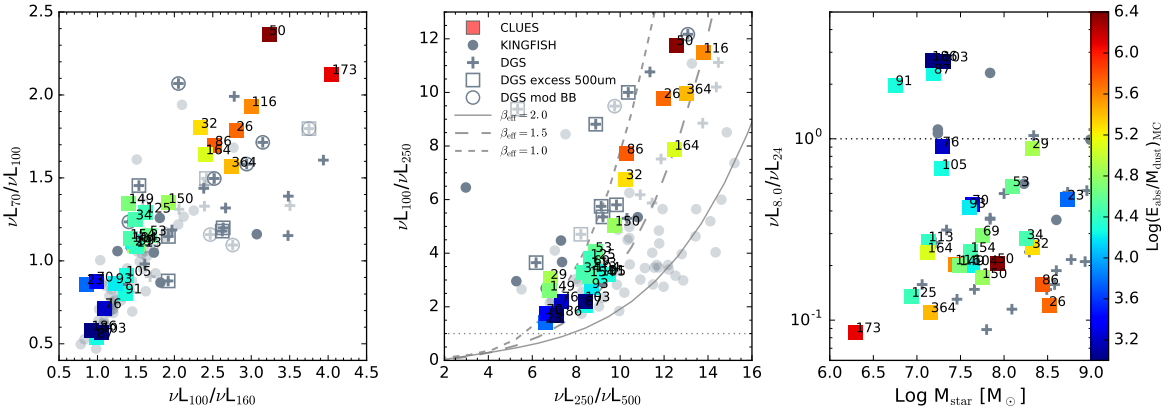

Figure 2: *Left:* The PACS/PACS diagram which traces the peak of the SED. *Center:* The PACS/SPIRE diagram which reflects the variations of the emissivity index β. *Right:* Stellar mass vs. the L_8/L_{24} ratio which reflects the strengths of PAH emissions. Gray points: KINGFISH. Gray crosses: DGS. Colored squares: CLUES dwarf galaxies. The colorbar shows the amount of energy absorbed by MCs per unit dust mass.

Submm excess and slope flattening The central panel of Fig. 2 shows the PACS/SPIRE $\nu L_{100}/\nu L_{250}$ vs $\nu L_{250}/\nu L_{500}$ color-color diagram. This diagram reflects best the variations of β, the factor that modifies the slope of the submm part of the SED in a modified blackbody fit. The three lines show the theoretical luminosity ratios drawn from [9], calculated with blackbody fits of fixed β of 1, 1.5 and 2. The latter is the commonly used value for fitting data of normal, massive galaxies. We can see how certainly high mass galaxies follow the higher β, while dwarf galaxies, both observed and simulated, present smaller $\nu L_{250}/\nu L_{500}$ ratios, occupying the $1.0 < \beta < 1.5$ region and thus evidencing a general flattening of their submm slopes. Note the presence of those DGS galaxies marked in [9] as having an excess of emission at 500 μm (open squares). CLUES dwarfs with a dominant MC emission are the furthest away from the $\beta = 2$ line showing the highest luminosity ratios, while dwarfs with almost bare cirrus emission fall the closest. In fact, if we lower the t_0 value, the bulk of CLUES galaxies lose much of their MC emission steepening their submm slopes, which is reflected in an approach of their representative points to the $\beta = 2$ line.

Low PAH emission The $\nu L_{8.0}/\nu L_{24}$ ratio is a good estimator of the PAH peak intensities, since it compares the strength of one of the most prominent peaks among the aromatic features (8.6 μm) and the intensity at the nearest wavelength just out of the PAH spectral region. The right panel of Fig. 2 shows this IRAC 8μm/MIPS 24μm *Spitzer* luminosity ratio compared to stellar mass. We can see that CLUES dwarfs show very low PAH emission, the same as has been reported for DGS as well as for some KINGFISH dwarfs [11]. Only a couple of them with very poor MC emission (or low energy absorbed per unit mass in MCs) show a PAH emission that is higher than the average, but still consistent with data. We propose that the weakness or lack of PAH emission in DGS galaxies, is not only due to the low PAH abundance in low metallicity regions, but also caused by warm dust emission from PAH-deficient MCs

that partially or completely hides the cirri PAH features.

4 Conclusions

In this work we have studied the SEDs of a sample of simulated dwarf galaxies calculated using the GRASIL-3D radiative transfer code, which treats separately the dense (molecular clouds) and diffuse (cirrus) components of the gas phase. The SEDs obtained show that the interplay between the emission from these 2 components recovers the particular spectral features observed in the IR-submm region of samples such as DGS or HAPLESS: IR peak broadening, submm excess and low PAH emission. The driving parameter adequately describing these features is the amount of energy absorbed per unit dust mass in MCs, the energy coming from young stars. The lower this parameter, the less apparent the particular features are, recovering the high mass and metallicity galaxy behaviour in the lower limit.

Acknowledgments

We thank the CLUES collaboration for providing the initial conditions for the simulations analyzed in this work. We also thank MINECO, Spain, for financial support through grants AYA2012-31101 and MINECO/FEDER AYA2015-63810-P.

References

[1] Clark, C. J. R., Dunne, L., Gomez, H. L. et al. 2015, MNRAS, 452, 397-430

[2] Domínguez-Tenreiro, R., Obreja, A., Granato, G. L. et al. 2014, MNRAS, 439, 3868-3889

[3] Draine, B. T., Dale, D. A., Bendo, G. et al. 2007, ApJ, 663, 866-894

[4] Draine, B. T. and Li, A. 2007, ApJ, 657, 810-837

[5] Galliano, F., Madden, S. C., Jones, A. P. et al. 2003, A&A, 407, 159-176

[6] Gottloeber, S.,Hoffman, Y. and Yepes, G. 2010, arXiv.1005.2687

[7] Governato, F., Brook, C., Mayer, L. et al. 2010, Nature, 463, 203-206

[8] Granato, G. L. and Danese, L., 1994, MNRAS, 268, 235

[9] Rémy-Ruyer, A., Madden, S. C., Galliano, F., et al. 2013, A&A, 557, A95

[10] Rémy-Ruyer, A., Madden, S. C., Galliano, F., et al. 2014, A&A, 563, A31

[11] Rémy-Ruyer, A., Madden, S. C., Galliano, F., et al. 2015, A&A, 582, A121

[12] Schneider, N., Csengeri, T.,Hennemann, P. et al. 2012, A&A, 540, L11

[13] Silva, L.,Granato, G. L., Bressan, A. and Danese, L. 1998, ApJ, 509, 103-117

[14] Stinson, G., Seth, A., Katz, N., Wadsley, J. et al. 2006, MNRAS, 373, 1074-1090

[15] Vega, O., Silva, L., Panuzzo, P. et al. 2005, MNRAS, 364, 1286-1298

[16] Wada, K., Norman, C. A. 2007, ApJ, 660, 276-287

[17] Wadsley, J. W., Stadel, J. and Quinn, T. 2004, NewA, 9, 137-158